Supporting Information

Facile synthesis of Cu(II)-Mn(II) complexes by using a new Cu(II) complex of an unsymmetrical ligand as O_3 donor metalloligand: Structures, magnetic properties, and catalytic oxidase activities

Sabarni Dutta[a], Júlia Mayans[b] and Ashutosh Ghosh[a,*]

[a]*Department of Chemistry, University College of Science, University of Calcutta, 92, A.P.C. Road, Kolkata 700 009, India, E-mail address: ghosh_59@yahoo.com*

[b]*Departament de Química Inorgànica I Orgànica, Secció Inorgànica and Institut de Nanosciència I Nanotecnologia (IN²UB). Martíi Franqués 1-11. 08028, Barcelona, Spain.*

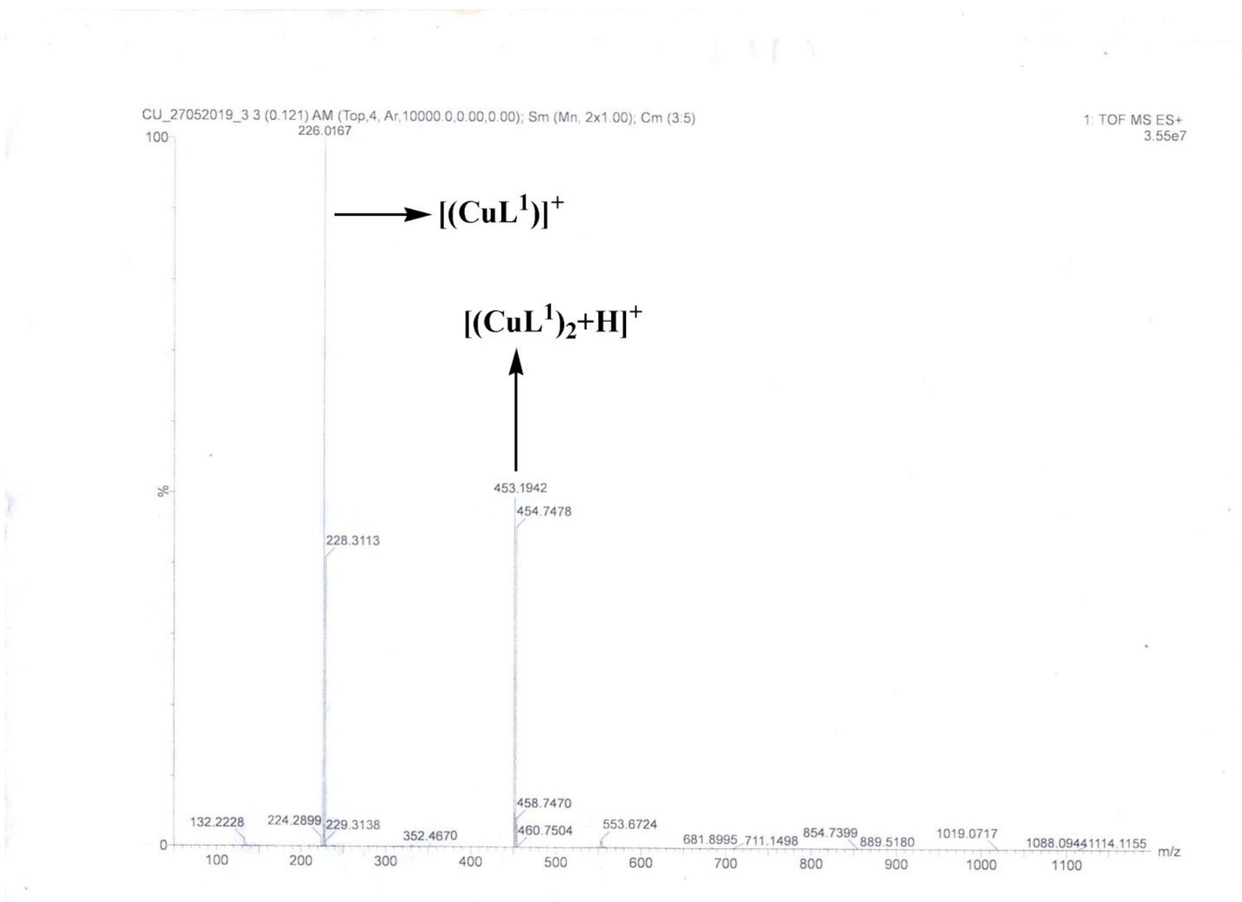

Fig. S1. Representative ESI mass spectrum of mono condensed complex $[CuL^1Im]ClO_4^-$.

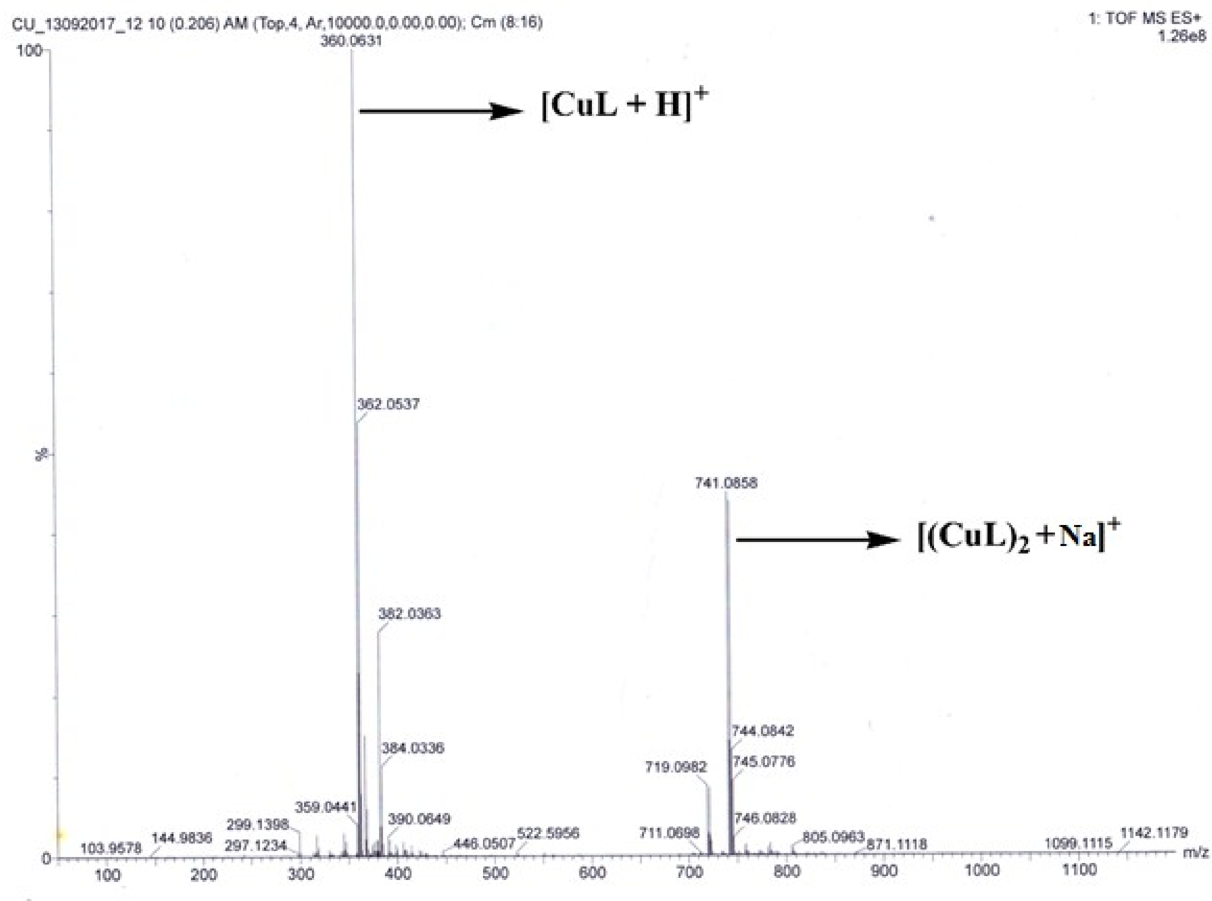

Fig. S2. Representative ESI mass spectrum of complex **1.**

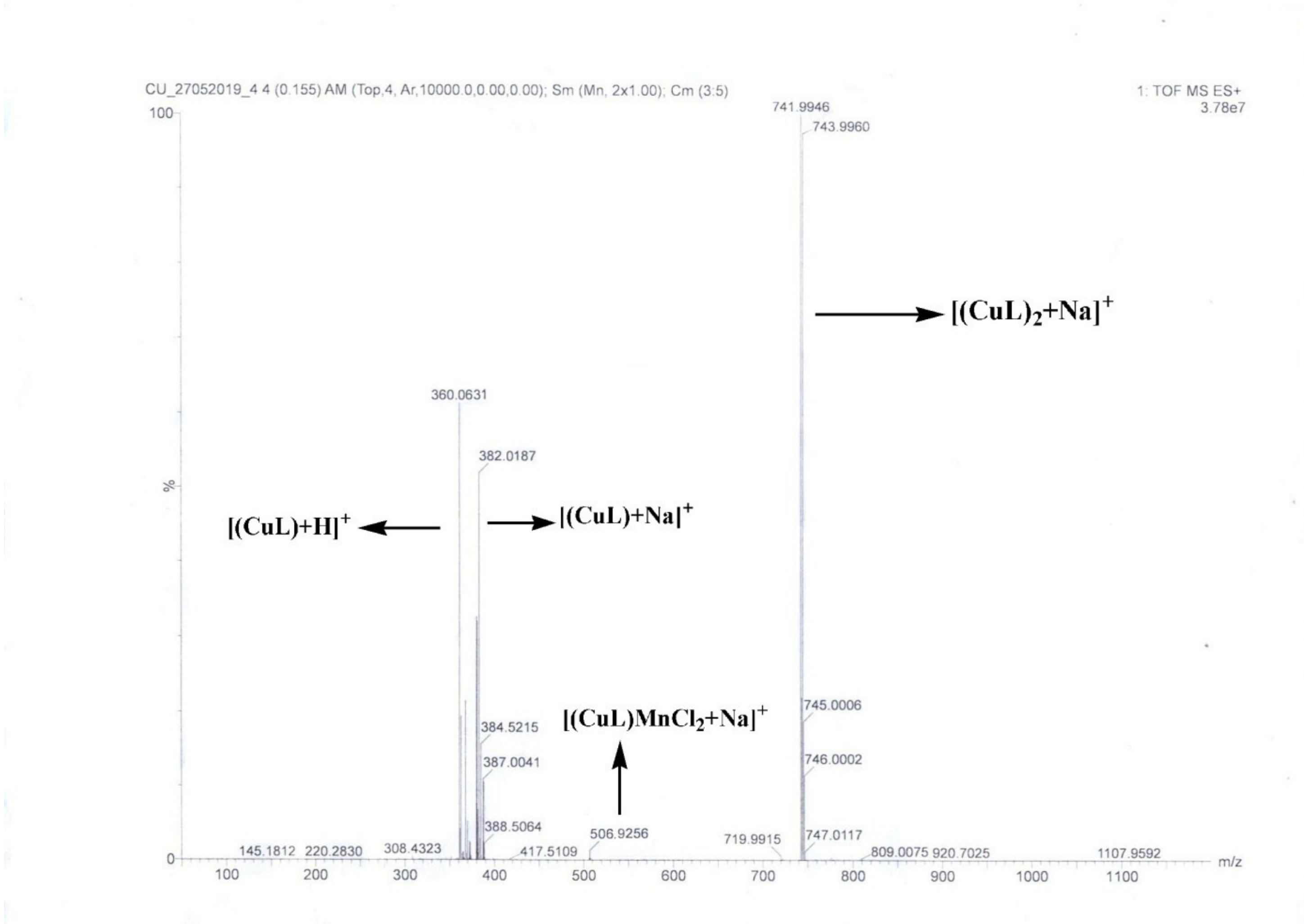

Fig. S3. Representative ESI mass spectrum of complex **2**.

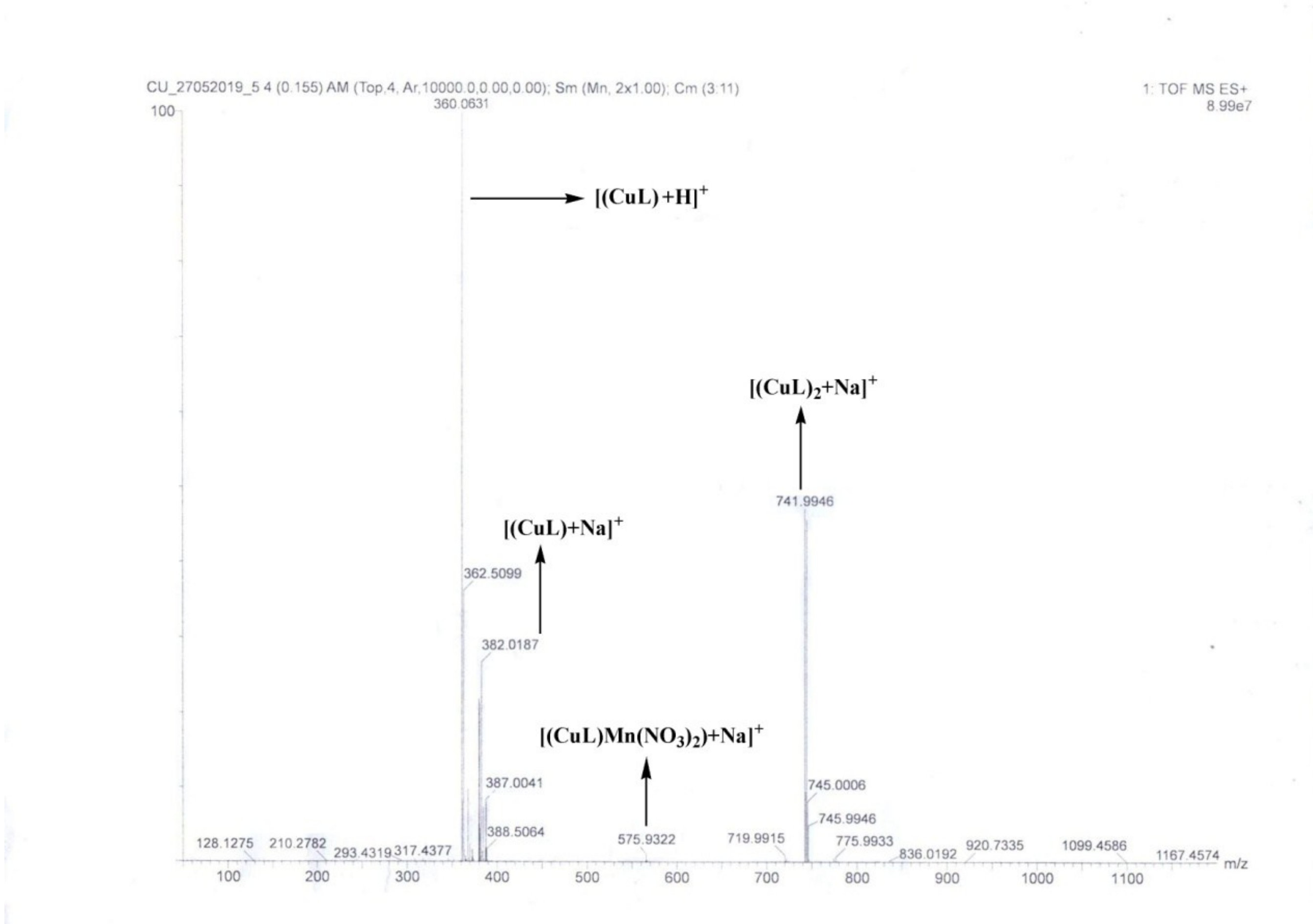

Fig. S4. Representative ESI mass spectrum of complex **3**.

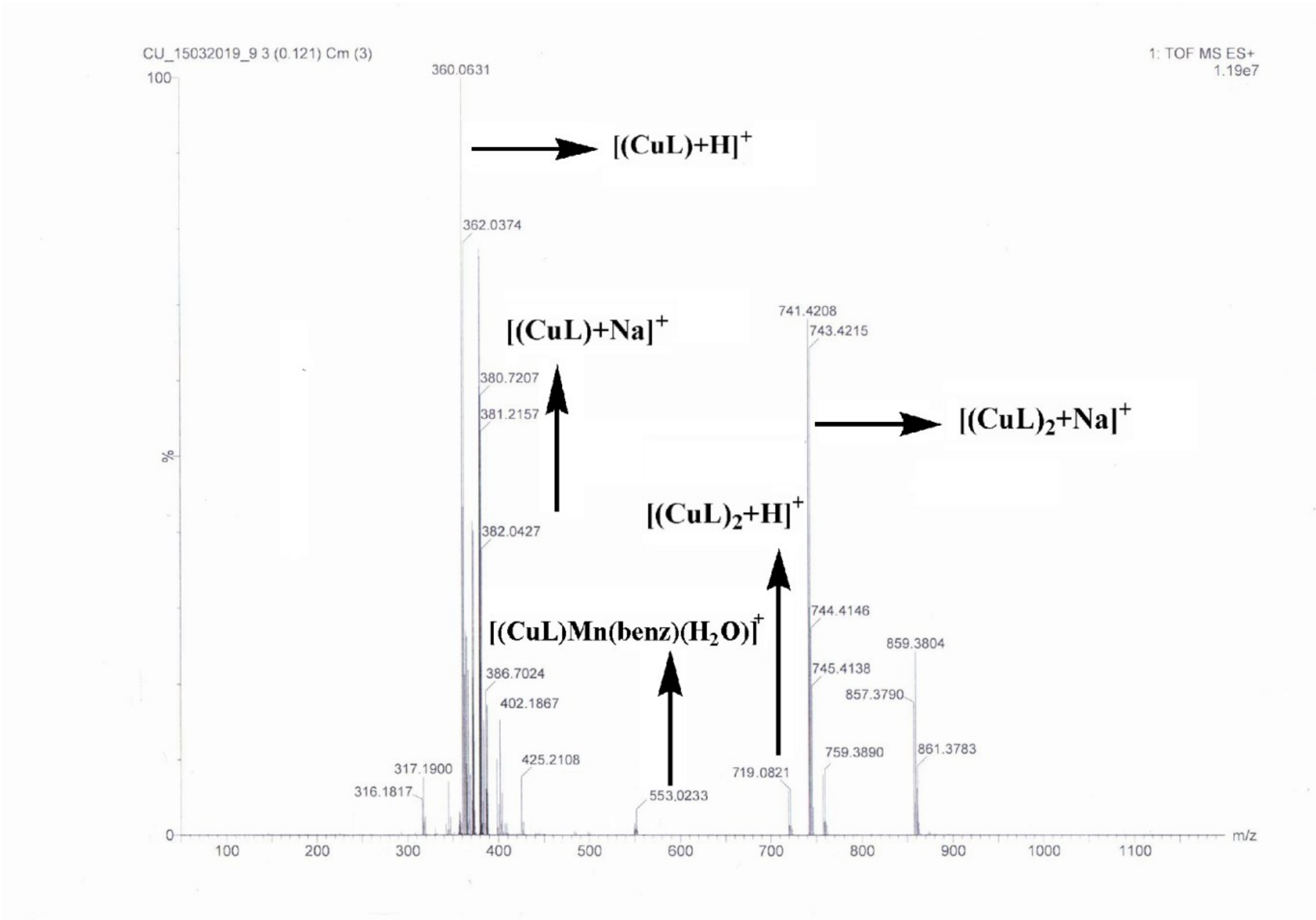

Fig. S5. Representative ESI mass spectrum of complex **4**.

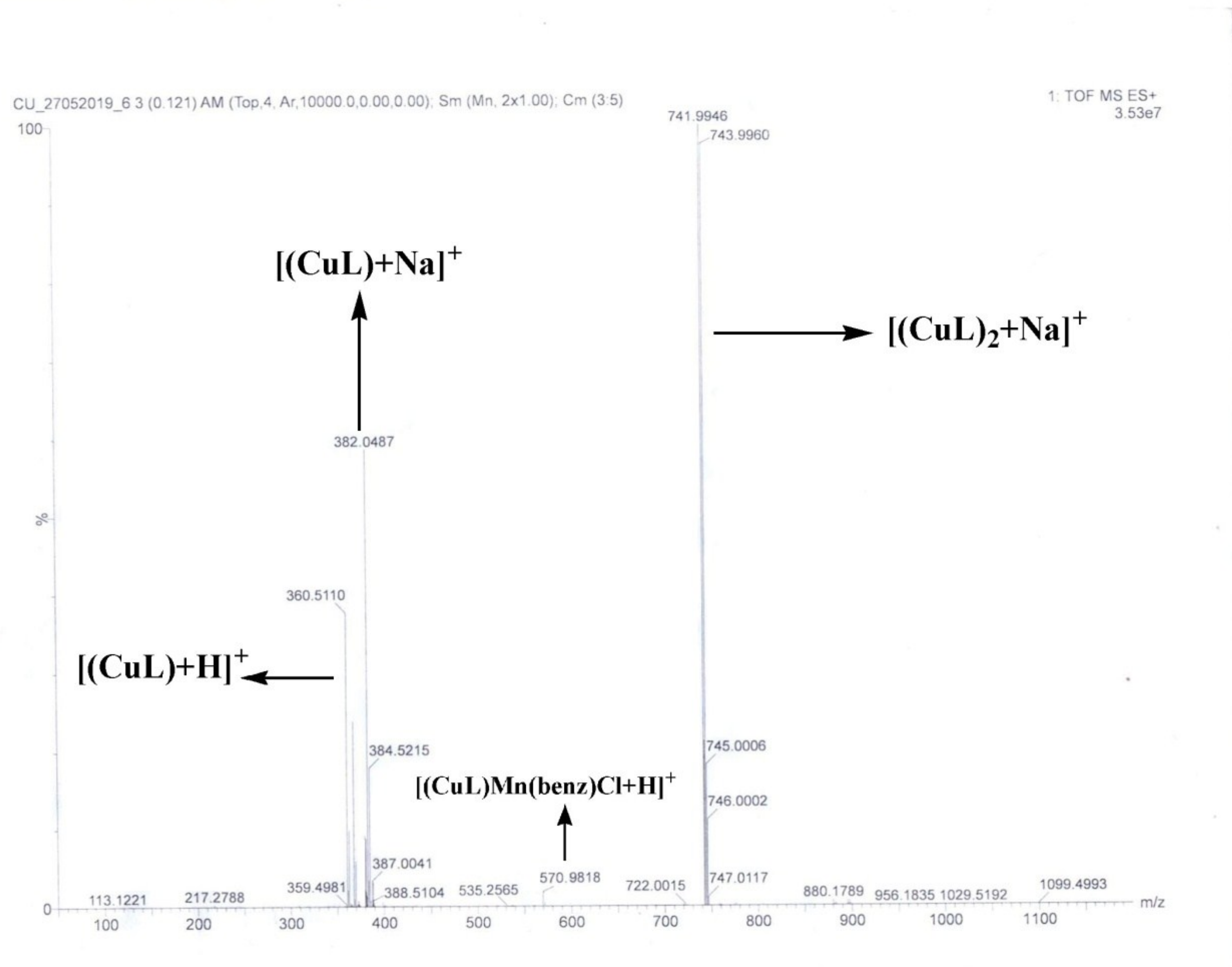

Fig. S6. Representative ESI mass spectrum of complex **5**.

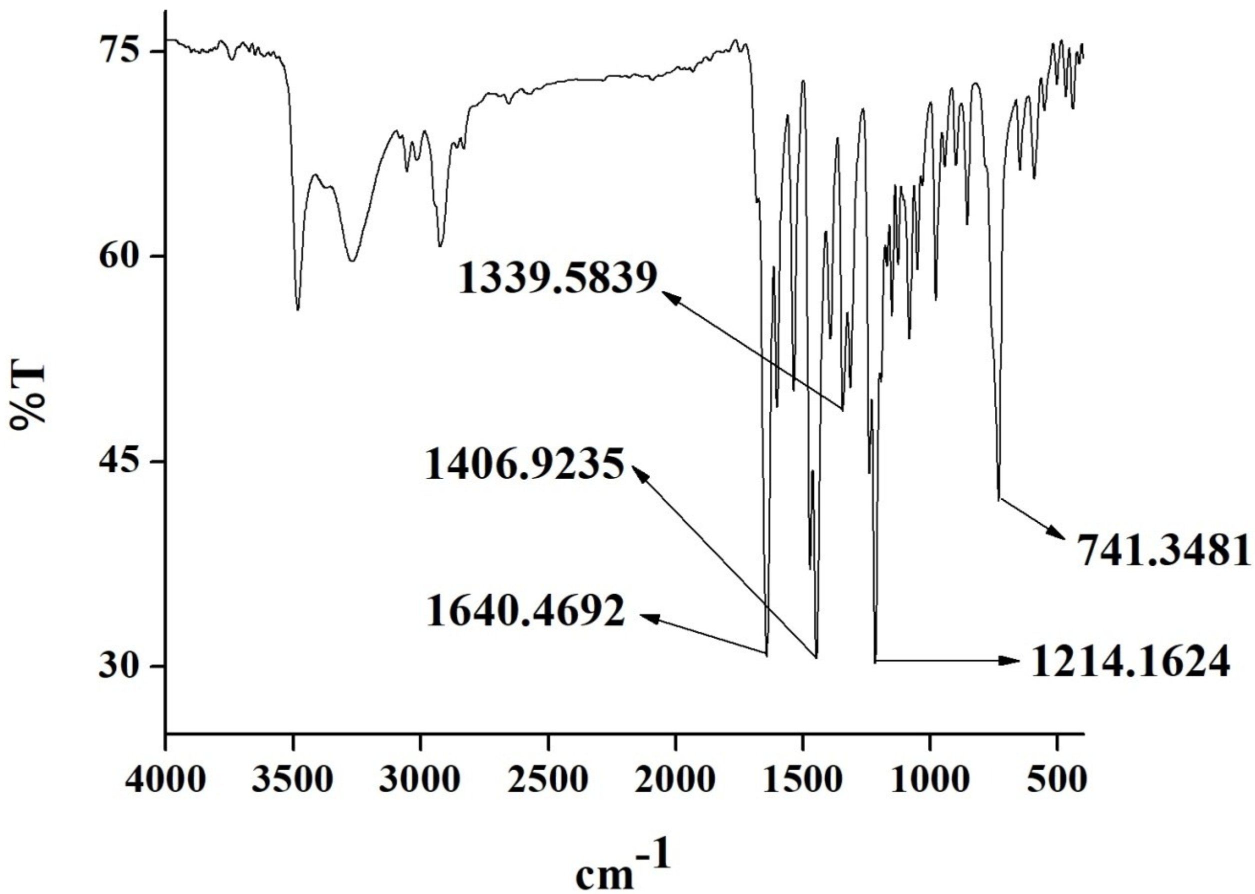

Fig. S7. Representative IR spectrum of Complex **1.**

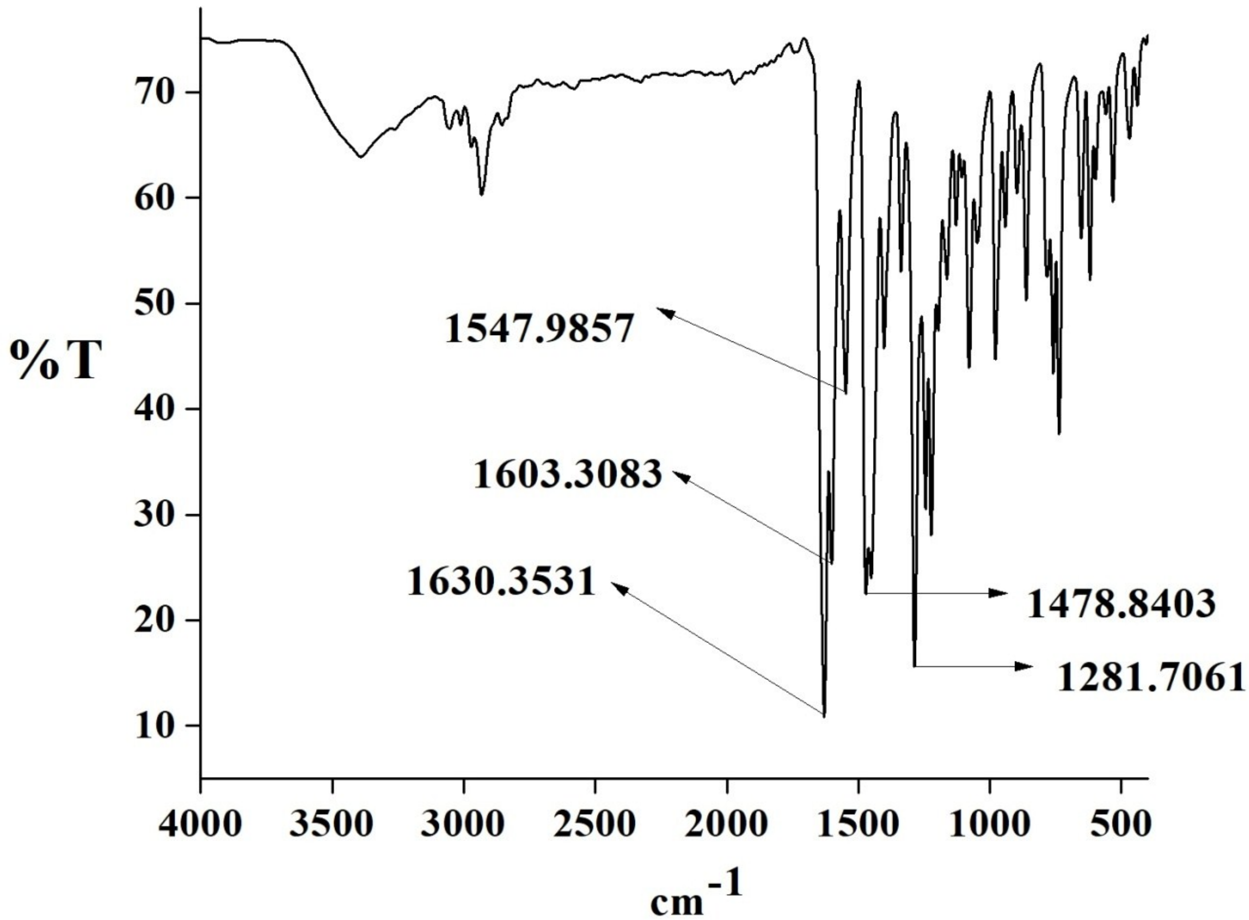

Fig. S8. Representative IR spectrum of Complex **2.**

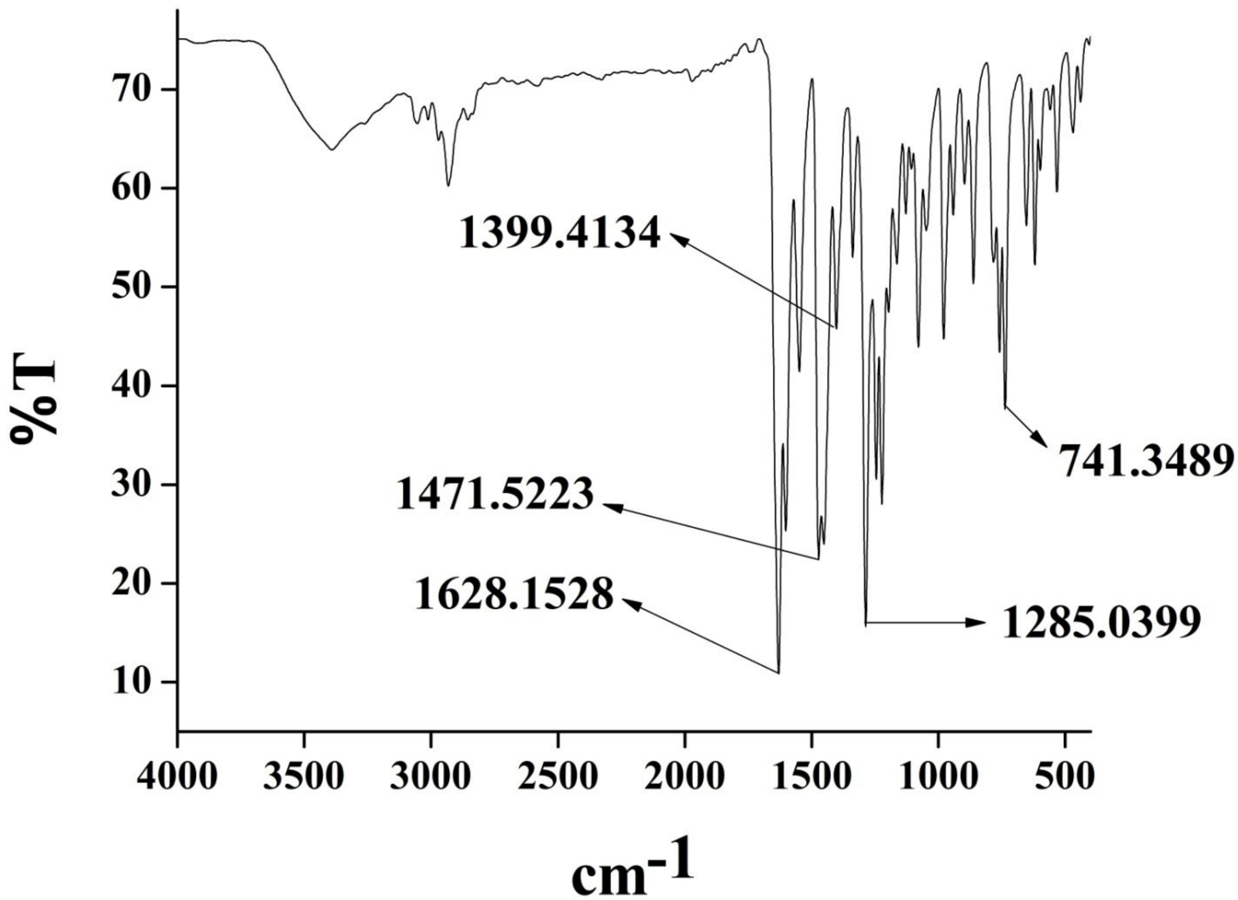

Fig. S9. Representative IR spectrum of Complex **3.**

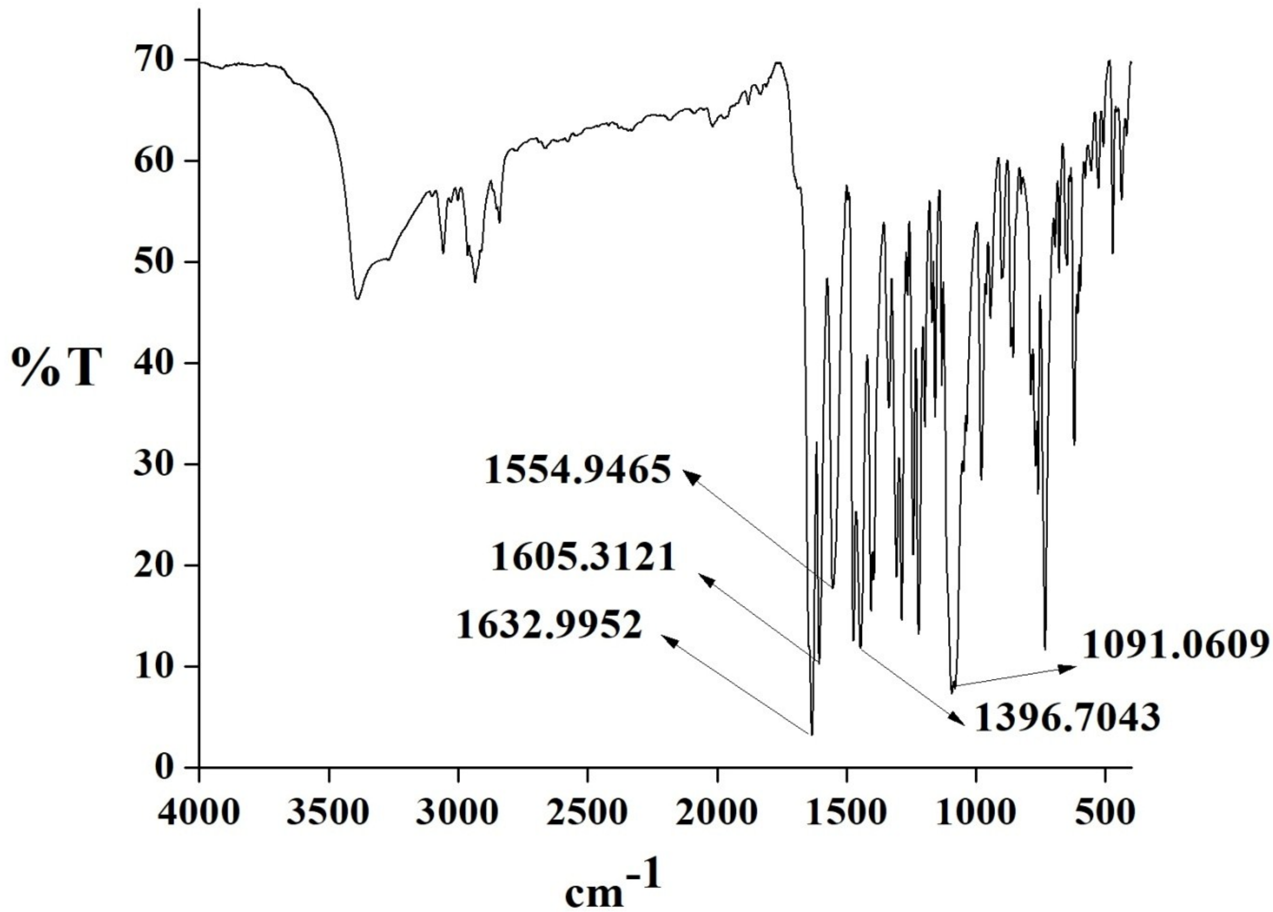

Fig. S10. Representative IR spectrum of Complex **4.**

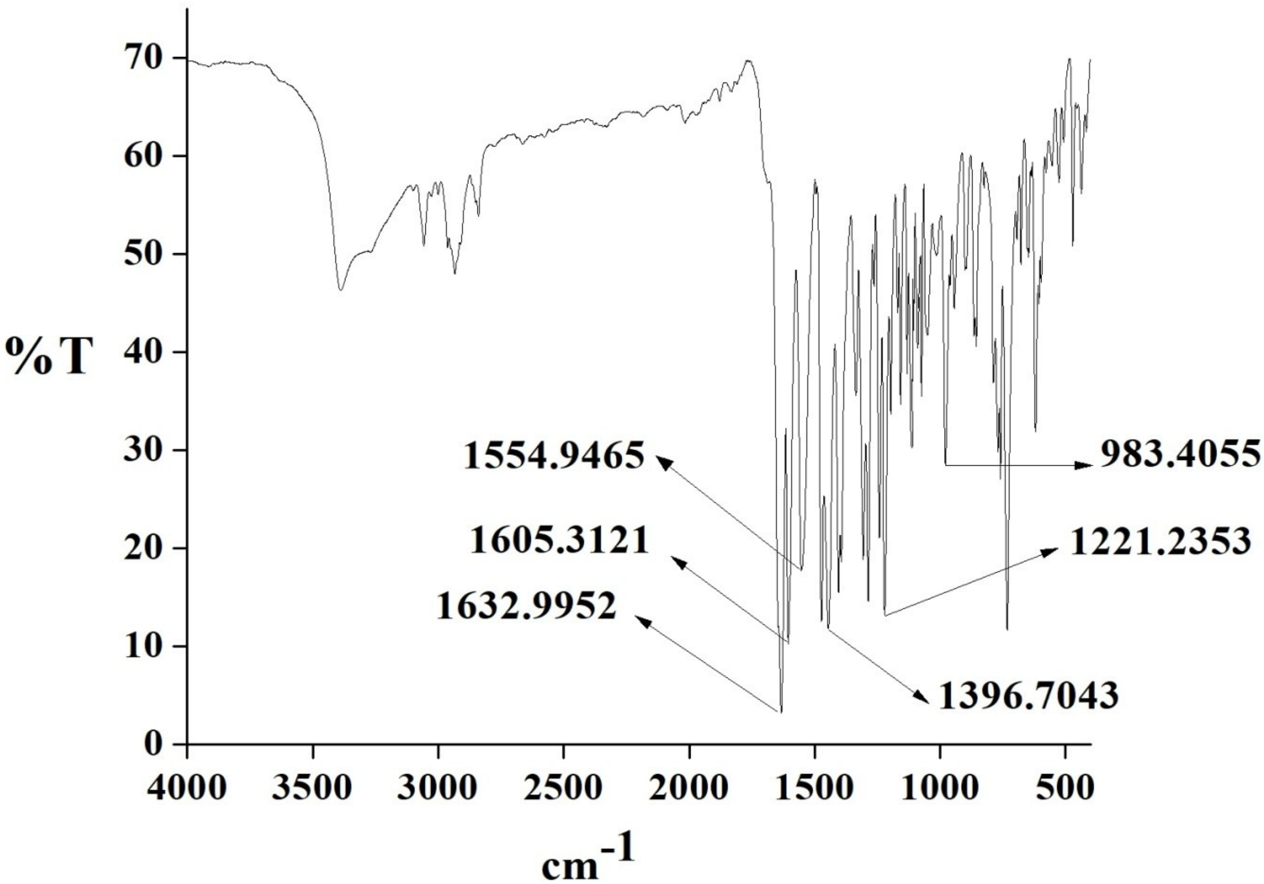

Fig. S11. Representative IR spectrum of Complex **5.**

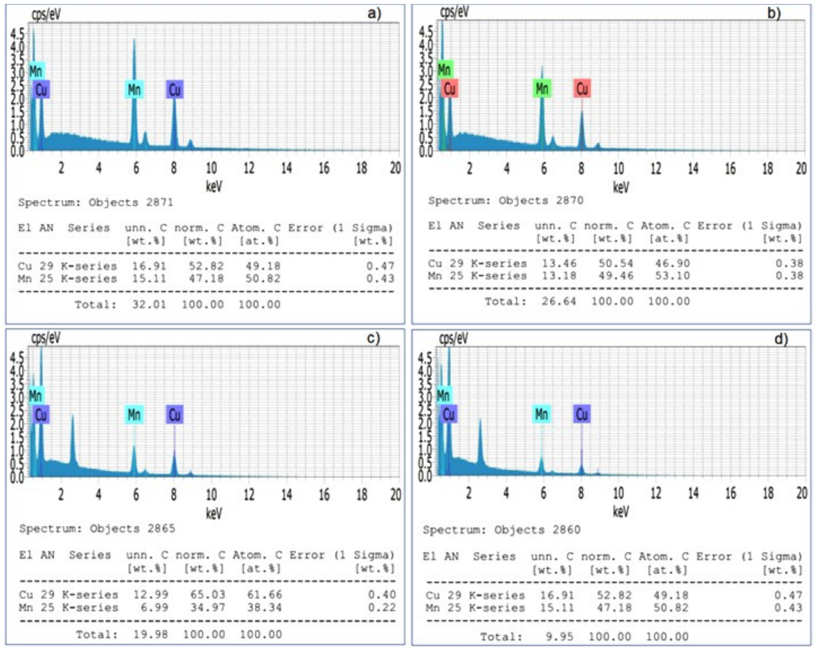

Fig. S12. The EDX spectrum and data of the synthesized complexes **2**−**5** (a−d).

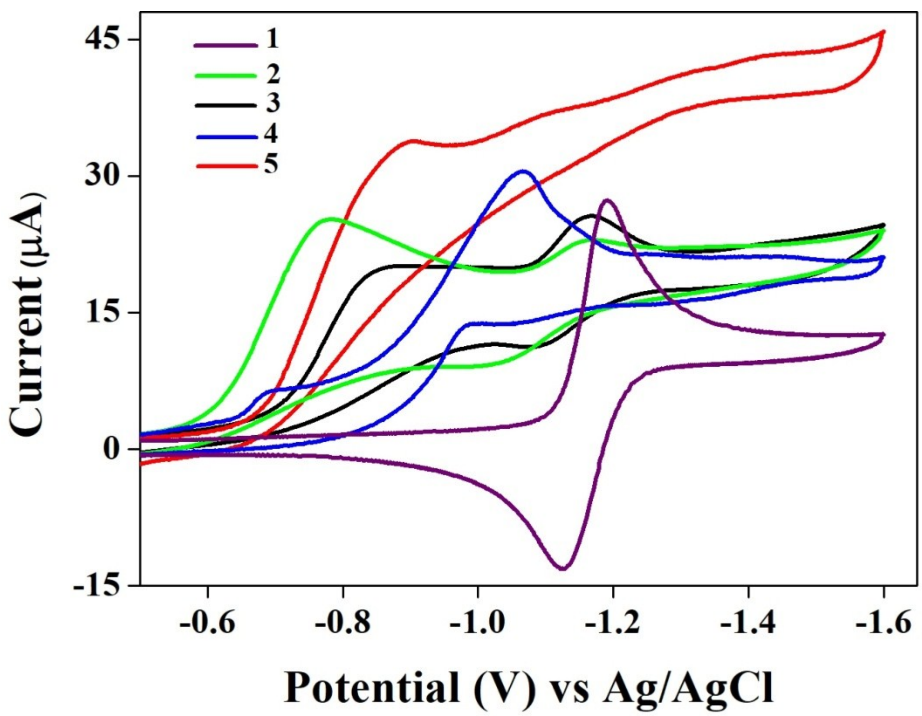

Fig. S13. Cyclic voltammograms (CVs) of 10^{-3} M solution of complexes **1**−**5** in acetonitrile at room temperature and a scan rate of 100 mV/Sec, using TBAP as supporting electrolyte.

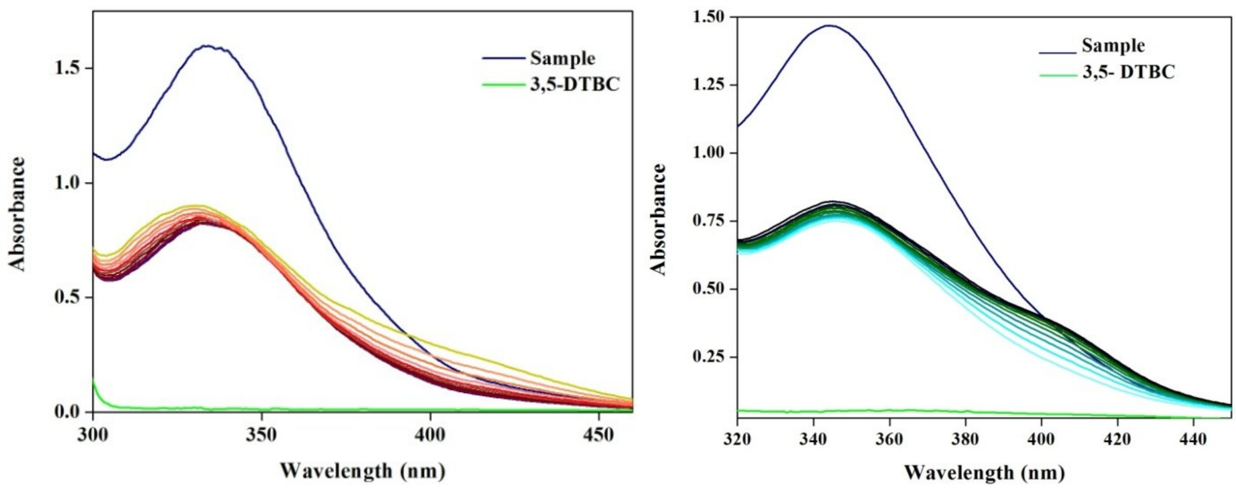

Fig. S14. Increase in the 3,5- DTBQ band at around 395 nm after the addition of 100 equiv of 3,5-DTBC to an acetonitrile solution of complexes **2** (left) and **3** (right). The spectra were recorded at 3 mins interval.

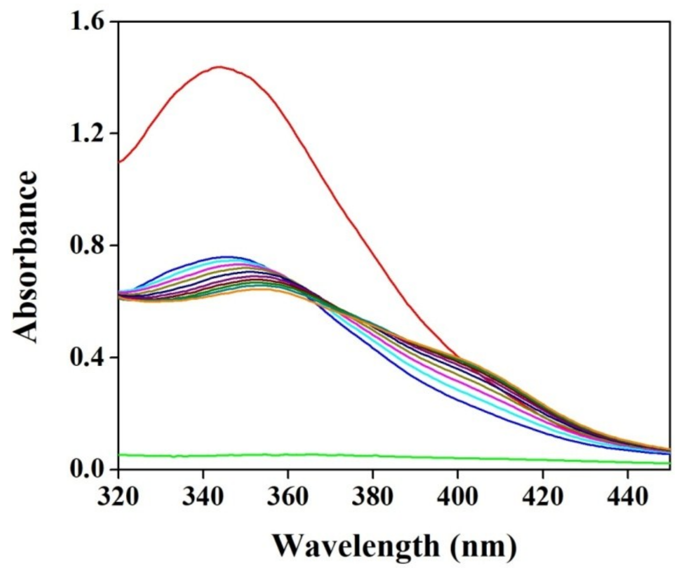

Fig. S15. Increase in the 3,5- DTBQ band at around 395 nm after the addition of 100 equiv of 3,5-DTBC to an acetonitrile solution of complex **5**. The spectra were recorded at 3 mins interval.

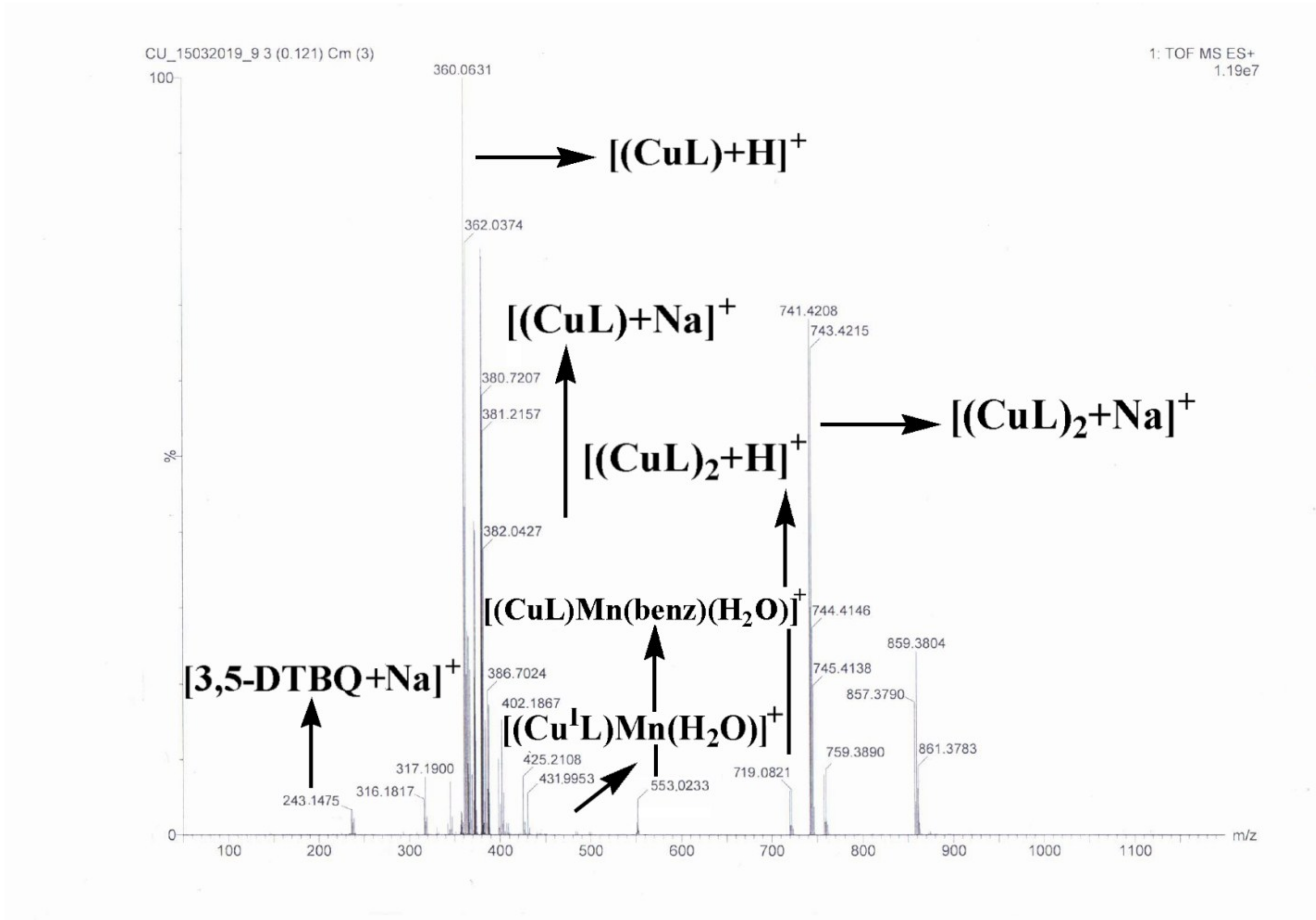

Fig. S16. Representative ESI mass spectrum of complex **4** with 3,5-DTBC.

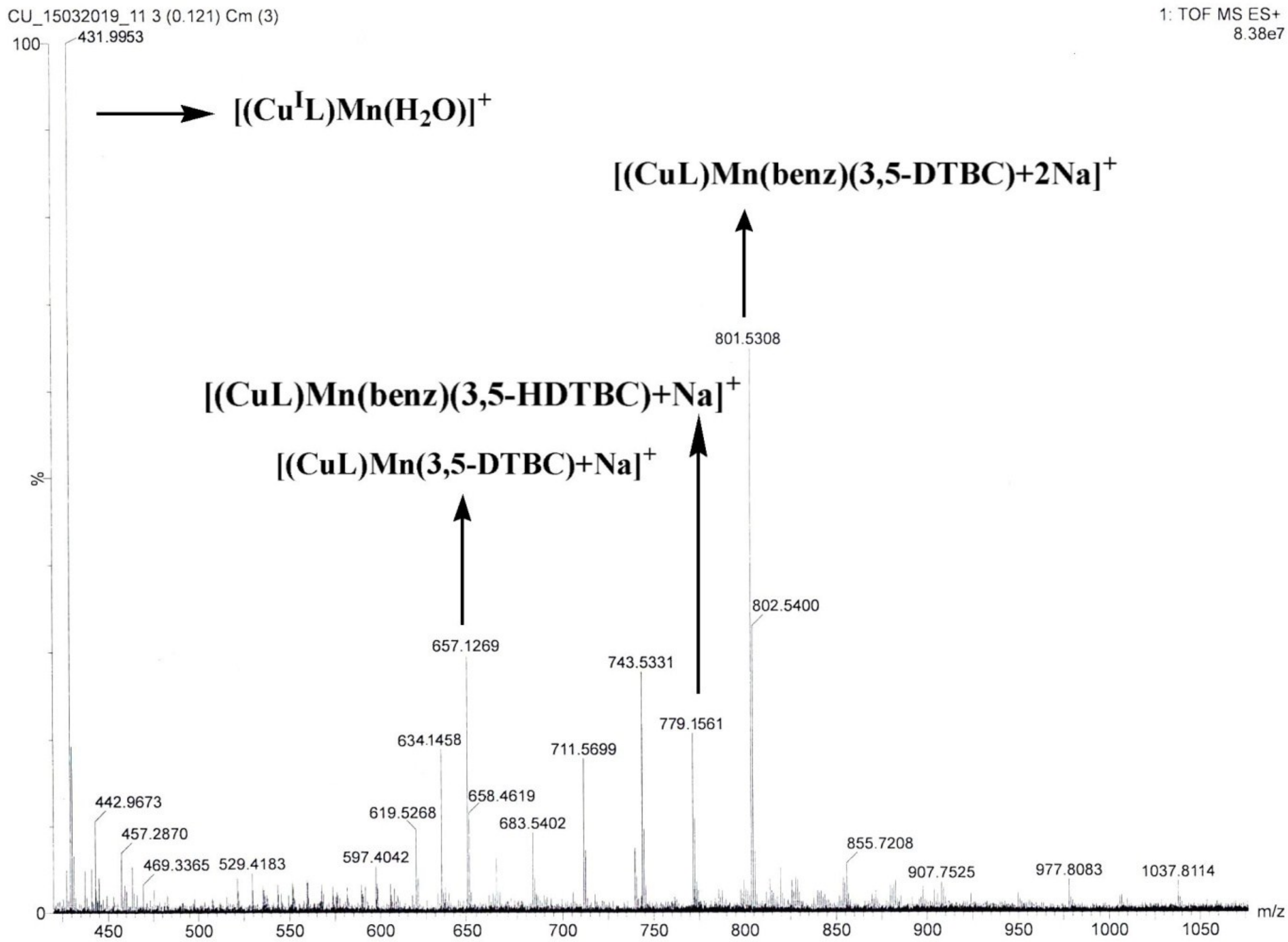

Fig. S17. Representative ESI mass spectrum of complex **4** with 3,5-DTBC.

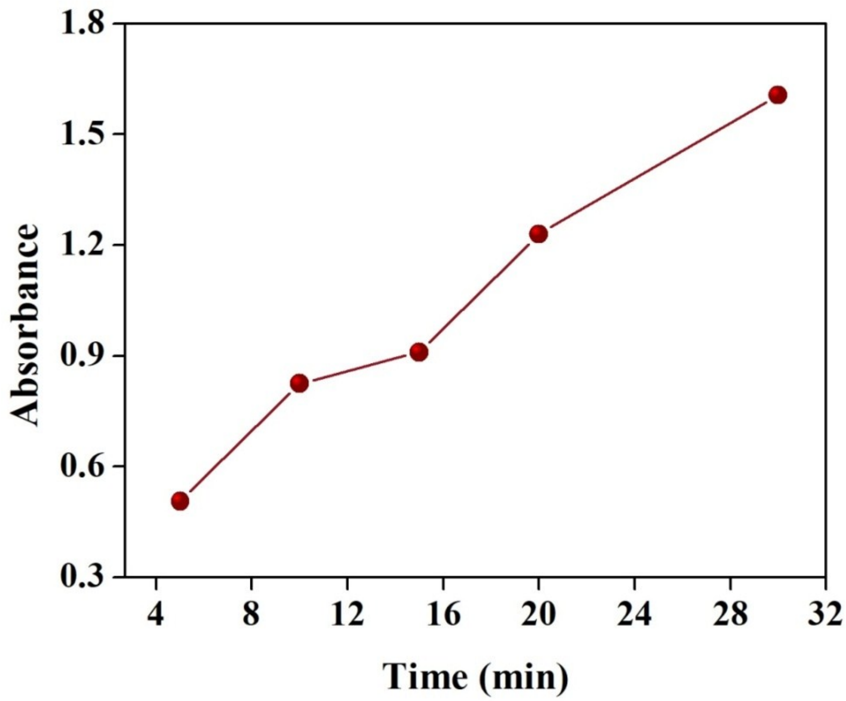

Fig. S18. Plot of absorption maxima at around 353 nm with different time (min).

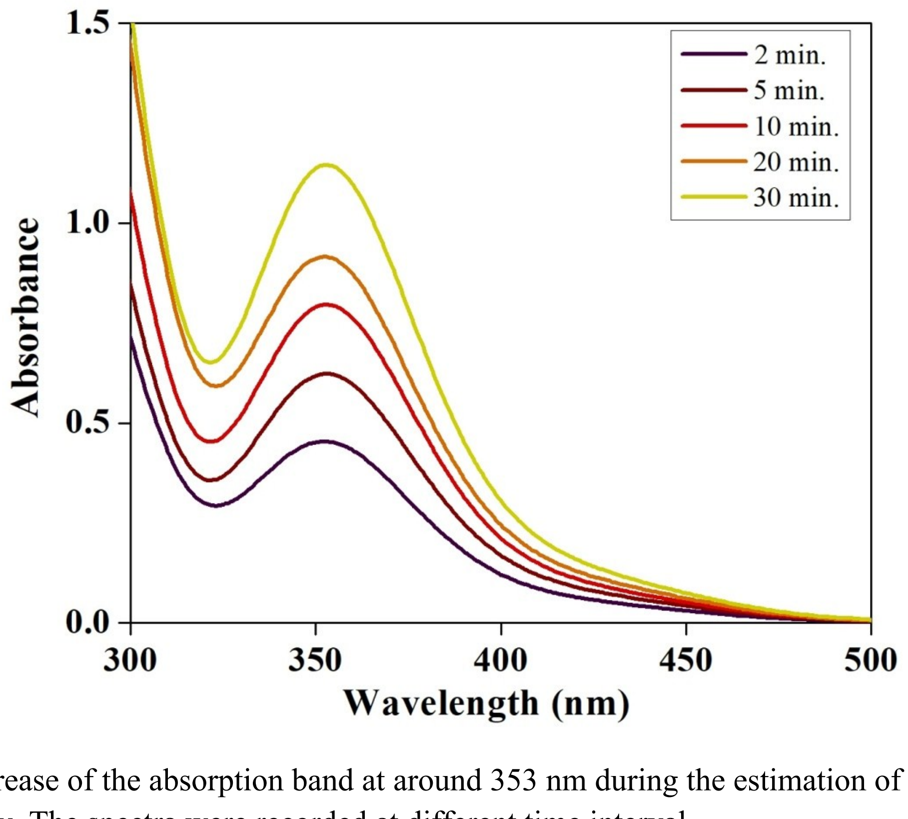

Fig. S19. Increase of the absorption band at around 353 nm during the estimation of H_2O_2 iodometrically. The spectra were recorded at different time interval.

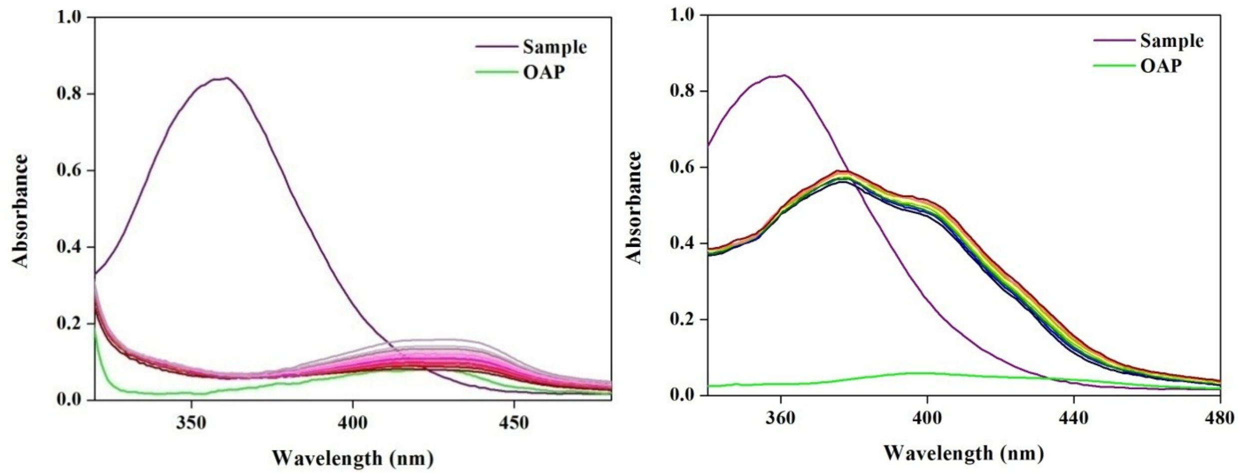

Fig. S20. Increase in the APX band at around 426 nm after the addition of 100 equiv of 2-aminophenol to an acetonitrile solution of complexes **2** (left) and **3** (right). The spectra were recorded at 3 mins interval.

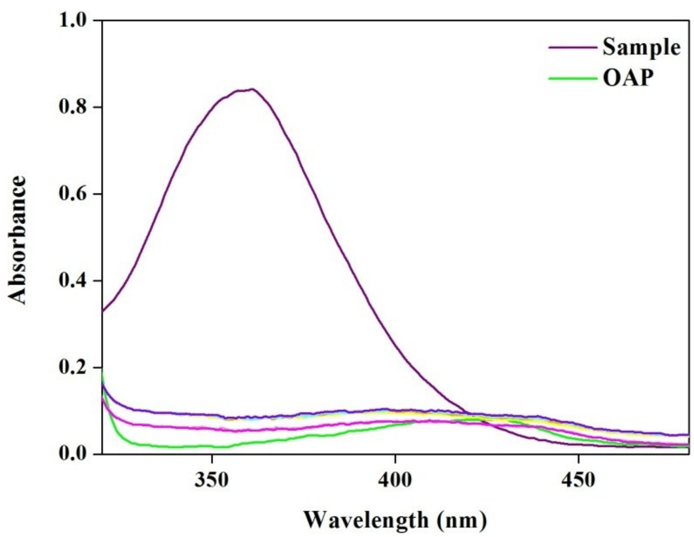

Fig. S21. Increase in the APX band at around 426 nm after the addition of 100 equiv of 2-aminophenol to an acetonitrile solution of complex **5**. The spectra were recorded at 3 mins interval.

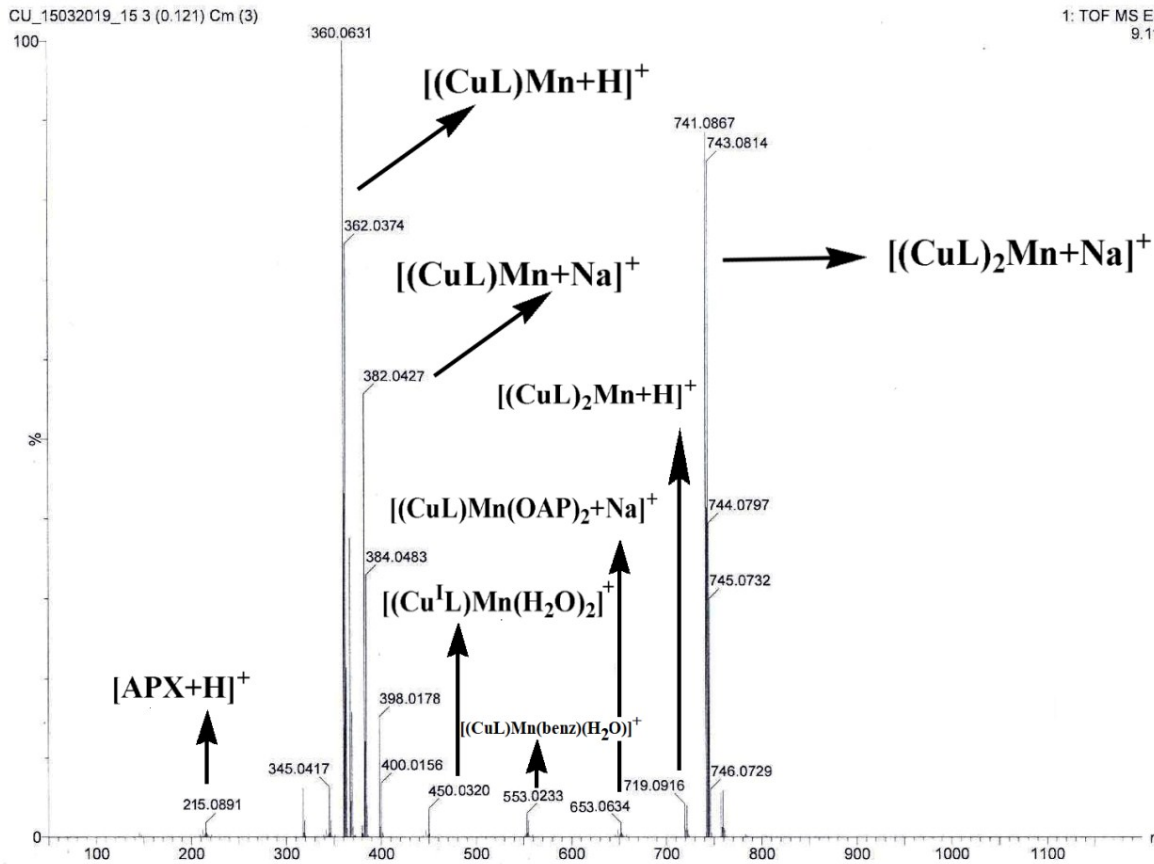

Fig. S22. Representative ESI mass spectrum of complex **4** with OAP.

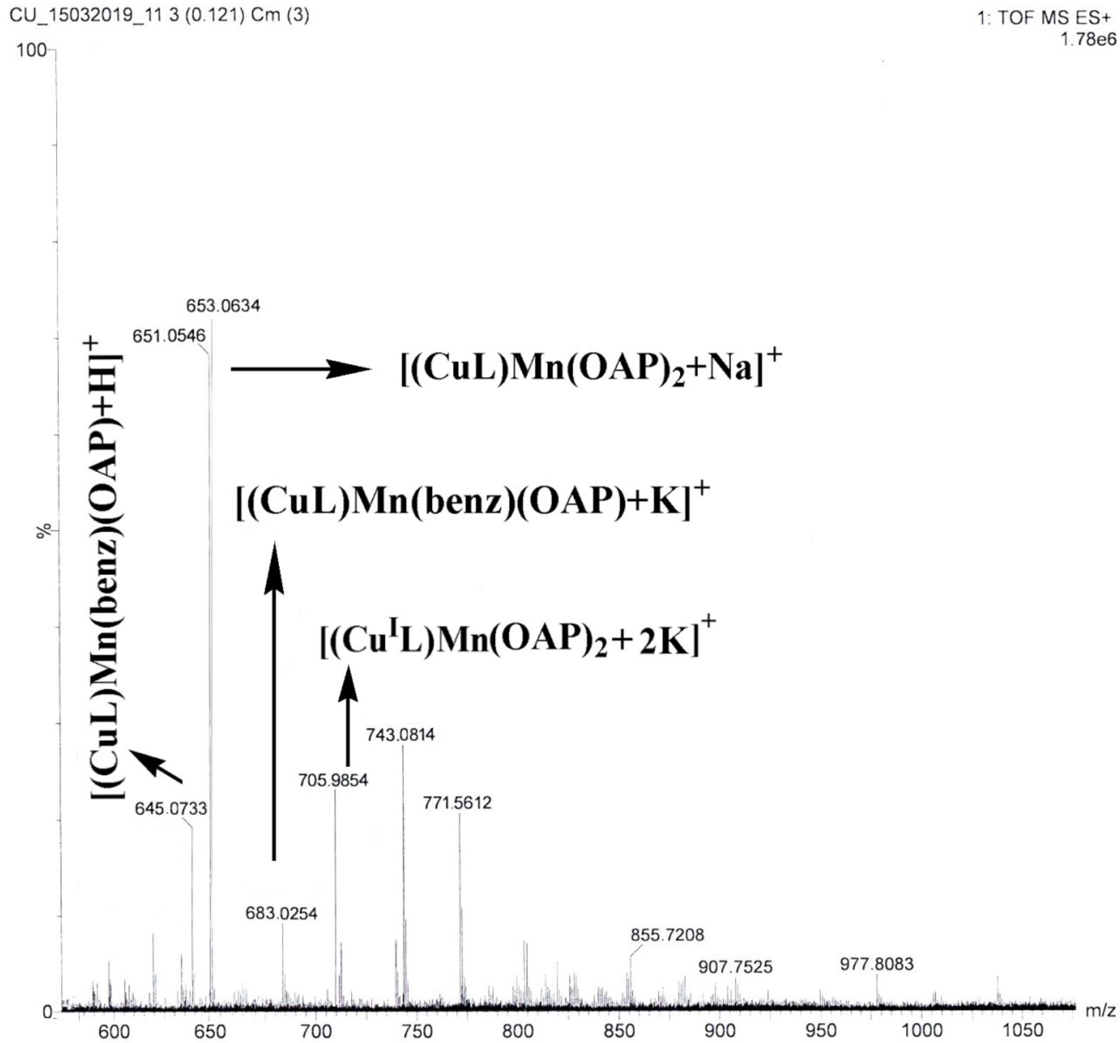

Fig. S23. Representative ESI mass spectrum of complex **4** with OAP.

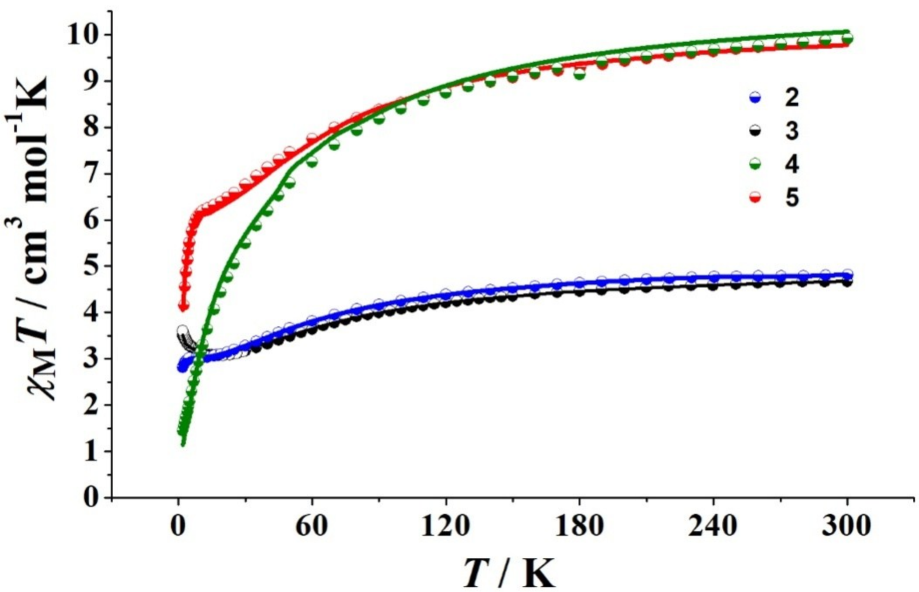

Fig. S24. Representation of the χT as a function of T for complexes **2** (black)**, 3**(blue)**, 4** (green) and **5** (red). Solid lines represent the best fit for each product.

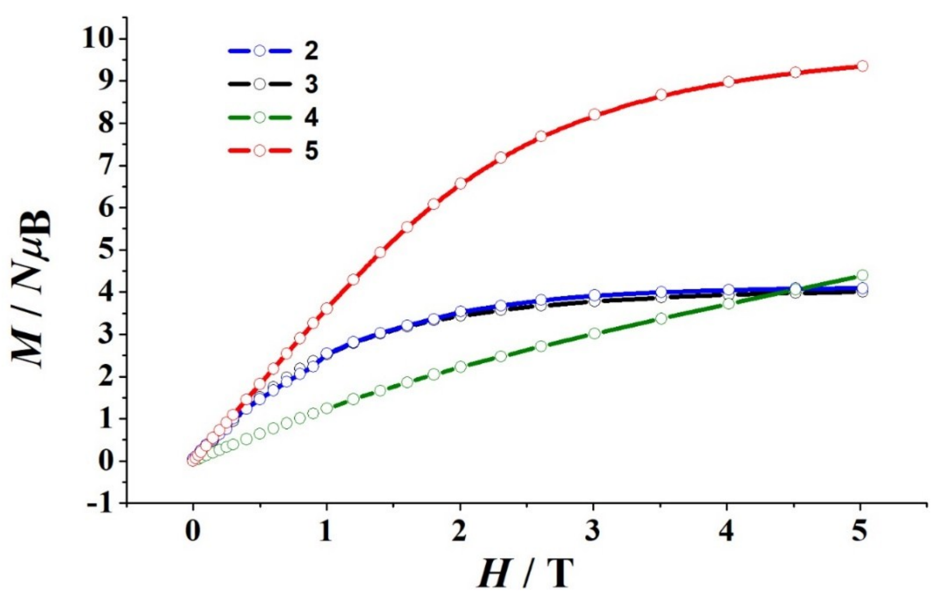

Fig. S25. Representation of the magnetization curves for complexes **2** (blue)**, 3** (black)**, 4** (green) and **5** (red).

Table S1: Bond distances (Å) and angles (°) for complex **2**.

Bond length (Å) of complex **2**			
Cu(1)−O(10)	1.897(8)	Mn(1)−Cl(2)	2.309(4)
Cu(1)−O(29)	1.891(8)	Mn(1)−O(10)	2.218(8)
Cu(1)−N(18)	1.898(10)	Mn(1)−O(29)	2.091(8)
Cu(1)−N(21)	1.920(2)	Mn(1)−O(30)	2.450(10)
Mn(1)−Cl(1)	2.299(5)		
Bond angle (°) of Complex **2**			
O(10)−Cu(1)−O(29)	83.8(3)	Cl(1)−Mn(1)−O(30)	94.9(3)
O(10)−Cu(1)−N(18)	95.9(4)	Cl(2)−Mn(1)−O(10)	106.5(3)
O(10)−Cu(1)−N(21)	176.2(4)	Cl(2)−Mn(1)−O(29)	109.9(3)
O(29)−Cu(1)−N(18)	177.6(5)	Cl(2)−Mn(1)−O(30)	94.7(3)
O(29)−Cu(1)−N(21)	94.3(4)	O(10)−Mn(1)−O(29)	71.9(3)
N(18)−Cu(1)−N(21)	85.9(4)	O(10)−Mn(1)−O(30)	138.1(3)
Cl(1)−Mn(1)−Cl(2)	114.49(2)	O(29)−Mn(1)−O(30)	67.0(3)
Cl(1)−Mn(1)−O(10)	107.7(3)	Cu(1)−O(10)−Mn(1)	99.4(3)
Cl(1)−Mn(1)−O(29)	133.2(3)	Cu(1)−O(29)−Mn(1)	104.2(4)

Table S2: Bond distances (Å) and angles (°) for complex **3**.

Bond length (Å) of Complex **3**			
Cu(1)−O(10)	1.902(4)	Mn(1)−O(29)	2.121(5)
Cu(1)−O(29)	1.907(5)	Mn(1)−O(30)	2.502(4)
Cu(1)−N(18)	1.917(7)	Mn(1)−O(32)	2.312(6)
Cu(1)−N(21)	1.919(7)	Mn(1)−O(34)	2.320(6)
Cu(1)−O(39)[a]	2.643(7)	Mn(1)−O(36)	2.361(7)
Mn(1)−O(10)	2.329(5)	Mn(1)−O(40)	2.195(4)
Bond angle (°) of Complex **3**			
O(10)−Cu(1)−O(29)	85.38(2)	O(10)−Mn(1)−O(30)	136.87(2)
O(10)−Cu(1)−N(18)	95.0(3)	O(34)−Mn(1)−O(10)	144.34(2)

O(10)−Cu(1)−N(21)	178.3(2)	O(34)−Mn(1)−O(29)	140.22(2)
O(10)−Cu(1)−O(39)[a]	95.0(2)	O(34)−Mn(1)−O(30)	75.12(2)
O(29)−Cu(1)−N(18)	175.7(2)	O(34)−Mn(1)−O(40)	82.7(2)
O(29)−Cu(1)−N(21)	94.4(3)	O(34)−Mn(1)−O(36)	112.9(2)
O(29)−Cu(1)−O(39)[a]	84.7(3)	O(10)−Mn(1)−O(36)	74.8(2)
N(18)−Cu(1)−N(21)	85.2(3)	O(10)−Mn(1)−O(40)	82.11(2)
O(39)[a]−Cu(1)−N(18)	99.5(3)	O(29)−Mn(1)−O(30)	66.50(2)
O(39)[a]−Cu(1)−N(21)	86.6(3)	O(29)−Mn(1)−O(36)	90.9(2)
O(32)−Mn(1)−O(10)	96.35(2)	O(29)−Mn(1)−O(40)	87.28(2)
O(32)−Mn(1)−O(29)	166.0(2)	O(30)−Mn(1)−O(36)	110.9(2)
O(32)−Mn(1)−O(30)	126.76(2)	O(30)−Mn(1)−O(40)	90.20(2)
O(32)−Mn(1)−O(34)	53.8(2)	O(36)−Mn(1)−O(40)	156.0(2)
O(32)−Mn(1)−O(36)	80.2(2)	Cu(1)−O(10)−Mn(1)	98.20(2)
O(32)−Mn(1)−O(40)	96.51(2)	Cu(1)−O(29)−Mn(1)	105.55(2)
O(10)−Mn(1)−O(29)	70.78(2)		

Where [a] = −1/2 + x, 1/2 − y, −1/2 + z.

Table S3: Bond distances (Å) and angles (°) for complex **4**.

Bond length (Å) of Complex **4**			
Cu(1)−O(10)	1.910(3)	Cu(2)−O(41)	1.905(3)
Cu(1)−O(29)	1.885(3)	Mn(1)−O(10)	2.268(3)
Cu(1)−N(18)	1.891(5)	Mn(1)−O(29)	2.145(3)
Cu(1)−N(21)	1.922(5)	Mn(1)−O(30)	2.478(3)
Cu(2)−N(52)	1.913(4)	Mn(1)−O(32)	2.094(3)
Cu(2)−N(49)	1.938(4)	Mn(1)−O(40)[a]	2.122(3)
Cu(2)−O(60)	1.893(3)	Mn(1)−O(1)	2.197(4)
Bond angle (°) of Complex **4**			
O(10)−Cu(1)−O(29)	84.51(2)	O(1)−Mn(1)−O(30)	86.58(2)
O(10)−Cu(1)−N(18)	96.68(2)	O(1)−Mn(1)−O(32)	83.18(2)

O(10)−Cu(1)−N(21)	174.58(2)	O(10)−Mn(1)−O(29)	70.59(2)
O(29)−Cu(1)−N(18)	176.04(2)	O(10)−Mn(1)−O(30)	136.79(2)
O(29)−Cu(1)−N(21)	94.07(2)	O(10)−Mn(1)−O(32)	137.43(2)
N(18)−Cu(1)−N(21)	85.1(2)	O(10)−Mn(1)−O(40)[a]	90.19(2)
O(41)−Cu(2)−N(52)	172.89(2)	O(29)−Mn(1)−O(30)	66.27(2)
O(60)−Cu(2)−N(49)	169.54(2)	O(29)−Mn(1)−O(32)	149.91(2)
O(60)−Cu(2)−N(52)	93.35(2)	O(29)−Mn(1)−O(40)[a]	95.89(2)
N(49)−Cu(2)−N(52)	84.12(2)	O(30)−Mn(1)−O(32)	84.69(2)
O(41)−Cu(2)−O(60)	90.54(2)	O(30)−Mn(1)−O(40)[a]	96.22(2)
O(41)−Cu(2)−N(49)	93.13(2)	O(32)−Mn(1)−O(40)[a]	94.88(2)
O(1)−Mn(1)−O(40)[a]	176.46(2)	Cu(1)−O(10)−Mn(1)	99.69(2)
O(1)−Mn(1)−O(10)	89.29(2)	Cu(1)−O(29)−Mn(1)	105.04(2)
O(1)−Mn(1)−O(29)	87.27(2)		

Where [a] = $1-x, 1-y, 1-z$.

Table S4: Bond distances (Å) and angles (°) for complex **5**.

Bond length (Å) of Complex **5**			
Cu(1)−O(10)	1.905(3)	Mn(1)−O(29)	2.108(3)
Cu(1)−O(29)	1.891(4)	Mn(1)−O(30)	2.487(4)
Cu(1)−N(18)	1.911(4)	Mn(1)−O(32)	2.318(5)
Cu(1)−N(21)	1.922(4)	Mn(1)−O(40)	2.208(5)
Cu(1)−Cl(1)[a]	2.810(2)	Mn(1)−Cl(1)	2.344(2)
Mn(1)−O(10)	2.196(3)		
Bondangle (°) of Complex **5**			
O(10)−Cu(1)−O(29)	83.02(2)	Cl(1)−Mn(1)−O(40)	132.83(2)
O(10)−Cu(1)−N(18)	95.57(2)	O(10)−Mn(1)−O(29)	71.51(2)
O(10)−Cu(1)−N(21)	173.9(2)	O(10)−Mn(1)−O(30)	136.64(2)
Cl(1)[a] −Cu(1)−O(10)	99.05(2)	O(10)−Mn(1)−O(32)	91.37(2)
O(29)−Cu(1)−N(18)	168.55(2)	O(10)−Mn(1)−O(40)	107.08(2)
O(29)−Cu(1)−N(21)	94.16(2)	O(29)−Mn(1)−O(30)	66.20(2)

Cl(1)[a] −Cu(1)−O(29)	104.97(2)	O(29)−Mn(1)−O(32)	139.84(2)
N(18)−Cu(1)−N(21)	86.2(2)	O(29)−Mn(1)−O(40)	93.36(2)
Cl(1)[a]−Cu(1)−N(18)	86.52(2)	O(30)−Mn(1)−O(32)	127.59(2)
Cl(1)[a]−Cu(1)−N(21)	86.88(2)	O(30)−Mn(1)−O(40)	84.86(2)
Cl(1)−Mn(1)−O(10)	109.36(2)	O(32)−Mn(1)−O(40)	56.41(2)
Cl(1)−Mn(1)−O(29)	126.08(2)	Cu(1)[a]−Cl(1)−Mn(1)	117.31(6)
Cl(1)−Mn(1)−O(30)	88.70(10)	Cu(1)−O(10)−Mn(1)	100.23(2)
Cl(1)−Mn(1)−O(32)	93.65(2)	Cu(1)−O(29)−Mn(1)	103.96(2)

Where [a] = $1 - x, -y, 1 - z$.

Table S5: Geometrical features of hydrogen bonding interactions (distances (Å) and angles(°)) of Complex **4**.

D−H···A	**D−H**	**H···A**	**D···A**	**∠D−H···A**
O(1)–H(1A)···O(60)	0.84(3)	2.24(4)	2.818(4)	126(4)
O(1)–H(1A)···O(61)	0.84(3)	2.13(4)	2.918(6)	156(5)
O(1)–H(1B)···O(41)	0.84(4)	1.99(4)	2.804(5)	163(4)

Table S6. List of catecholase activities of various complexes on different solvents.

Complexes	**k_{cat} (h^{-1})**	**Solvent**	**References**
$[Cu_2(H_2L_A^2)(OH)(H_2O)(NO_3)](NO_3)_3\cdot 2H_2O$	32400	CH_3CN	1
$[Cu_2(L_A^1)(N_3)_3]$	28800	CH_3CN	1
$[Cu_2(L_A^3)(OH)(H_2O)_2](NO_3)_2$	14400	CH_3CN	1
$[Cu(L_B^1)(H_2O)(NO_3)]_2$	10800	CH_3CN	1
$[Cu_2(L_C)_2(H_2O)_2]$	850, 694, 1003, 773	CH_3OH	2
$[Cu_2(L_C)_2(H_2O)_x]$	863, 785, 1080	CH_3OH	2
$[Cu_2(L_D)_2(H_2O)_2]$	2006, 883	CH_3OH	2

$[Cu_2(ClL_D)_2]\cdot 2H_2O$	3120	CH_3OH	2
$[Cu_2(L_E)_2(H_2O)_2]\cdot H_2O$	595	CH_3OH	2
$[Cu_2(L_F)_2(H_2O)_2]\cdot H_2O$	513	CH_3OH	2
$[Cu_2(L_G)_2(H_2O)_2]\cdot H_2O$	460	CH_3OH	2
$[Cu_2L_H(N_3)_2\cdot 2H_2O]$	1800	CH_3OH	3
$[Cu_2L_I(N_3)_2\cdot 2H_2O]$	2160	CH_3CN	3
$[Cu_2L_J(N_3)_2\cdot 2H_2O]$	2820	CH_3OH	3
$[Cu_2L_J(N_3)_2\cdot 2H_2O]$	1080	CH_3CN	3
$[Cu_2L_K(N_3)_2\cdot 2H_2O]$	1800	CH_3OH	3
$[Cu_2L_L(N_3)_2\cdot 2H_2O]$	2160	CH_3CN	3
$[Cu_2L_L(N_3)_2\cdot 2H_2O]$	720	CH_3OH	3
$[Cu\text{-}(L_M)(H_2O)]$	2820	CH_3OH	4
$[Cu\text{-}(L_N)(H_2O)]$	2580	CH_3OH	4
$[Cu\text{-}(L_O)(H_2O)]$	1410	CH_3OH/DMSO	4
$[Cu\text{-}(L_P)(H_2O)]$	1800	CH_3OH/DMSO	4
$[Cu\text{-}(L_Q)(H_2O)]$	510	CH_3OH/DMSO	4
$[Cu\text{-}(L_R)(H_2O)]$	2760	CH_3OH/DMSO	4
$[Cu\text{-}(L_S)(H_2O)]$	3960	CH_3OH/DMSO	4
$[Mn(L_T)(H_2O)_3](NO_3)_2\cdot H_2O$	2160	CH_3OH	5

$[Mn(L_T)(SCN)_2(H_2O)]\cdot H_2O$	1440	CH_3OH	5
$[Mn(L_T)\{N(CN)_2\}(H_2O)_2](NO_3)\cdot H_2O$	720	CH_3OH	5
$[Mn^{II}(L_U)(H_2O)_3]^{2+}$	21600	CH_3OH	6
$[Mn^{II}(L_U)(SCN)_2(H_2O)]$	14400	CH_3OH	6
$[Mn^{II}(L_U)\{N(CN)_2\}(H_2O)_2]^+$	7200	CH_3OH	6
$[(CuL_V)_2Mn(N_3)(H_2O)](ClO_4)\cdot H_2O$	1118	CH_3OH	8a
Complex **4**	1251.85	CH_3CN	This work

where, L_B = 2-formyl-4-methyl-6R-iminomethyl-phenolato and L_A = 2,6-bis(R-iminomethyl)-4-methyl-phenolato; for L_B^1 and L_A^1, R = *N*-propylmorpholine; for L_A^2, R = *N*-ethylpiperazine; for L_A^3, R = *N*-ethylpyrrolidine, and for L_B^4, R = *N*-ethylmorpholine.

H_2L_C = 1-[(2-hydroxy-5-R-benzyl)amino]cyclopentane-1-carboxylic acid; R = H, Cl, CH_3, OH; R = H and x = 1, R = Cl and x = 2, R = CH_3 and x = 2.

H_2L_D = 2-[(2-hydroxy-5-R-benzyl)amino]cyclohexane-1-carboxylic acid; R = H, CH_3.

H_3L_E = *N*-(2,5-dihydroxybenzyl)-L-alanine.

H_3L_F = *N*-(2,4-dihydroxybenzyl)-L-alanine.

H_3L_G = *N*-(2,3-dihydroxybenzyl)-L-alanine.

H_2L_H = condensation product of 4-methyl-2,6-diformylphenol with 1,3-diaminopropane, H_2L_I = 1,2-diaminoethane, (H_2L_J) = 1,2-diaminopropane, (H_2L_K) = 1,2-diamino-2-methylpropane and (H_2L_L) = 1,2- diaminocyclohexane.

L_M = L-alanine and 2-hydroxybenzaldehyde, L_N = L-alanine and 2-hydroxy-5-methoxybenzaldehyde, L_O = L-alanine and 2-hydroxy-5-chlorobenzaldehyde, L_P = L-alanine and 2-hydroxy-5-bromobenzaldehyde, L_Q = L-glycine and 2-hydroxy-5- bromobenzaldehyde, L_R = L-valine and 2-hydroxy-5-bromobenzaldehyde and L_S = L-leucine and 2-hydroxy-5-bromobenzaldehyde

L_T = 2,6-bis{2-(N-ethyl)pyridineiminomethyl}-4-methylphenolato

L_U = Sgly (**1**), D-Sala (**2**), L-Sala (**3**), DL-Sala (**4**), Sab2 (**5**), Sbal (**6**), Sab4 (**7**), Sval (**8**), Shis (**9**), Styr (**10**) and Stryp (**11**)

H_2L_V = *N*-(2-hydroxyacetophenylidene)-*N*′-salicylidene-1,3-propanediamine

1 K. S. Banu, T. Chattopadhyay, A. Banerjee, S. Bhattacharya, E. Suresh, M. Nethaji, E. Zangrando and D. Das, *Inorg. Chem.*, 2008, **47**, 7083−7093.

2 B. Sreenivasulu, F. Zhao, S. Gao and J. J. Vittal, *Eur. J. Inorg. Chem.*, 2006, **2006**, 2656−2670.

3 K. S. Banu, T. Chattopadhyay, A. Banerjee, S. Bhattacharya, E. Zangrando and D. Das, *J. Mol. Catal. A: Chem.*, 2009, **310**, 34−41.

4 Y. Thio, X. Yang and J. J. Vittal, *Dalton Trans.*, 2014, **43**, 3545−3556.

5 A. Guha, K. S. Banu, A. Banerjee, T. Ghosh, S. Bhattacharya, E. Zangrando and D. Das, *J. Mol. Catal. A: Chem.*, 2011, **338**, 51−57.

6 C.-T. Yang, M. Vetrichelvan, X. Yang, B. Moubaraki, K. S. Murray and J. J. Vittal, *Dalton Trans.*, 2004, 113−121.

8a P. Mahapatra, S. Ghosh, S. Giri, V. Rane, R. Kadam, M. G. B. Drew and A. Ghosh, *Inorg. Chem.*, 2017, **56**, 5105−5121.

Table S7. *J* parameter for all the reported complexes with a double phenoxo bridge according to the Spin-Hamiltonian $H=-2J\cdot S_1S_2$, (α + β)/2 and the torsion angle M(II)−O−Cu(II)−O.

CCDC name	J/cm^{-1}	(α + β)/2/deg	M^{II}-O-Cu^{II}-O torsion/deg
BICBIA	-15.9	102.66	9.01
BICCAT	-29.1	106.89	6.14
CEPPUL	-35.77	106.32	2.50
CEPPLIT	-24.2	105.04	12.47
CEPPOF	-22.77	103.45	10.29
CEPQAS	-19.83	100.19	2.42
DEXQUIT	-17.4	103.75	0.00

FAEPCU	-13.2	95.7	26.05
GAJXUM	-35.80	107.5	0.88
ILAKOV	-11.0	101.6	13.22
LEGJAI	-22.4	100.2	12.01
MIXLEL	-15.9	103.42	3.46
QEKFIW	-18.4	100.90	9.89
UNIPEJ	-30.0	100.47	8.52
VOBLAA	-48.9	105.98	3.42
YUVRAJ	-15.1	103.75	2.40
AGSD1	-13.5	101.5	6.2
AGSD2	-13.5	101.85	2.71
AGSD3	-12.6	102.32	3.63
AGSD4	-13.24	102.08	8.82